Journal of Geosciences, Earth and Planetary Systems

PRIME OPEN ACCESS

Volume 2, Issue 1

Research Article

Date of Submission: 10 Oct, 2025
Date of Acceptance: 16 Feb, 2026
Date of Publication: 27 Feb, 2026

Corn Water Productivity Assessments with Aerial Camera Onboard Drone by Modelling Surface and Aerodynamic Resistances

Antônio Teixeira[1*], Diego Loureiro[1], Richard Souza[1], Jlyel Cruz[1], Maria Gonzaga[1], Janice Leivas[1], Celina Takemura[2] and André Almeida[2]

[1]Federal University of Sergipe (UFS), São Cristóvão-SE, Brazil

[2]Embrapa Territory, Campinas-SP, Brazil

***Corresponding Author:** Antônio Teixeira, Federal University of Sergipe (UFS), São Cristóvão-SE, Brazil.

Citation: Teixeira, A., Loureiro, D., Souza, R., Cruz, J., Gonzaga, M., et al. (2026). Corn Water Productivity Assessments With Aerial Camera Onboard Drone By Modelling Surface And Aerodynamic Resistances. *J Geosci Earth Planet Syst*, 2(1), 01-17

Abstract

Aerial images taken from a camera onboard a drone were used for corn water productivity (WP) assessments in Northeast Brazil, by using a Mapir camera together with weather, biomass and productivity (P_r) data, modelling actual evapotranspiration (ET_a) and biomass production (BIO). The effects of different nitrogen (N) fertilization cover levels were analyzed showing that there were significant differences on WP components from the emergency (E) to physiological maturation (PM) crop stages (CS), however, stabilizing at N at 200 kg ha^{-1}. Above this level, farmers should lose money increasing risks of negative environmental impacts with more N leaching to the water table. The evaporative fraction (ET_f), i.e., the ratio of ET_a to reference evapotranspiration (ET_0), taken as a root-zone moisture indicator, presented the best correlation with BIO and Pr , but the fraction of the absorbed photosynthetically active radiation (fp), representing soil cover by the canopies, is also important through photosynthetic activity. Comparing P_r and the BIO, the highest determination coefficient at V6 (pant with six leaves), confirming that the potential of corn yield is already defined at this CS. The models applied showed potential for monitoring vegetation and water conditions in corn crops, allowing rational fertilization practices while maintained yield at sustainable water use, with the possibility for replication of the methods in other environmental conditions.

Keywords: Geotechnologies, Water and Vegetation Indices, Root-Zone Moisture, Yield Prediction

Introduction

Corn (Zea mays L.) is one of the most important agricultural crops worldwide, being essential for the Brazilian's food security. In Northeast Brazil, the crop is for both grain and silage and, more recently, for biofuel. Besides weather conditions, fertilization management drive actual evapotranspiration (ET_a) and biomass production (BIO), and then corn water productivity (WP), here considered as the ratio of BIO and productivity (Pr) to ET_a, being both indicators affected by root-zone moisture levels and the fraction of absorbed photosynthetically radiation. Among the several factors which drop corn WP under rainfed conditions, water deficit is the most important, mainly during the dry seasons [1-12]. Accounting the effect of N cover fertilization levels is relevant for corn commercial cultivation with sustainability because one of the ways to increase yield while minimizing environmental problems is through crop and water management improvements [1,2].

For monitoring the WP components during each crop stage, high spatial resolution images taken from aerial cameras onboard drones are effective tools for this task [2,4,13-16]. Besides crop management, root-zone moisture conditions affect the nutrient dynamics, thus, optimizing N cover fertilizations is important to increase corn WP [17]. The joint use of remote sensing and agrometeorological data can guide N fertilization managements retrieving ET_a and BIO, according to the N levels cover applied [2-4,6,17-22].

WP assessments in the current paper were done during the corn crop stages and for its growing season in the Atlantic Forest biome, Northeast Brazil, where for good corn yields, N cover fertilization is important for good yields, being urea is a common N source. However, urea applications in excess may promote environmental problems because part of this fertilizer may drain to the water table [2]. There are few remote sensing studies for modelling corn WP components in Brazil with high-resolution images with aerial cameras onboard drone involving distinct cultivars, biomes and crop managements [2,4]. Remote sensing algorithms have been elaborated and validated, inserting the Penman-Monteith (PM) equation to estimate ET_a [4,10,21,23-25].The SUREAL model based on the PM equation can be applied estimating the surface resistance (r_s), and the aerodynamic resistance (r_a) retrieved from roughness parameters [26,27]. SUREAL was elaborated with simultaneous remote sensing and field energy balance measurements involving distinct agroecosystems of Northeast Brazil under contrasting thermohydrological conditions, when it was named PM1 in this previous study and later tested and validated in other Brazilian regions [26,21].

To estimate corn BIO from aerial camera onboard drone in the current study, Monteith's radiation efficiency model (RUE) was applied [28]. The model is based on the interception of photosynthetically active radiation (PAR) by the canopies, which is variable throughout the crop stages [4,6,20,21,30]. To apply the RUE model, a specific value for corn maximum radiation use efficiency ε_{max} was used considering the effect of root-zone moisture through the evaporative fraction (ET_f) and checking the estimations with BIO field measured values [3,6,20,21,31]. Even that, the SUREAL and RUE models have been successfully applied for WP assessments in agricultural crops and natural vegetation in Brazil the development of aerial cameras onboard drone still demand applications with high resolution images to subsidize crop and water managements, mainly under the actual scenarios of climate and land-use changes. [21]

With ET_a estimated, BIO estimated and measured, together with field measurements of Pr WP assessments were carried out by using the visible and infrared bands of aerial images from a Mapir camera onboard a drone. The reference studied crop was a rainfed corn within the Atlantic Forest biome of Northeast Brazil, analyzing the effects of different N cover fertilization levels with urea N source along crop stages and for the growing season. The remote sensing derived parameters crossed with agrometeorological data were the Normalized Different Vegetation Index (NDVI), surface albedo (α_0) and surface temperature (T_0). Without thermal bands with the Mapir camera, T_0 was retrieved from the radiation balance equations applying the Stefan Boltzmann law, assuming the low atmosphere and the Earth surface emitting longwave radiation as back bodies [3,21]. The authors believe that the results have potential for recommendation of N fertilization management when aiming at corn WP improvements under different N cover fertilizing levels and root-zone moisture conditions and that, from the success of the applications, the models should be replicated in other environmental and crop conditions with simple calibrations of the modelling equations.

Material and Methods

Study Area, Crop Stages And Fertilization Managements

Figure. 1 shows the experimental area with corn plots cover fertilized by different nitrogen (N) levels, in the São Cristóvão County, Sergipe State, Northeast Brazil.

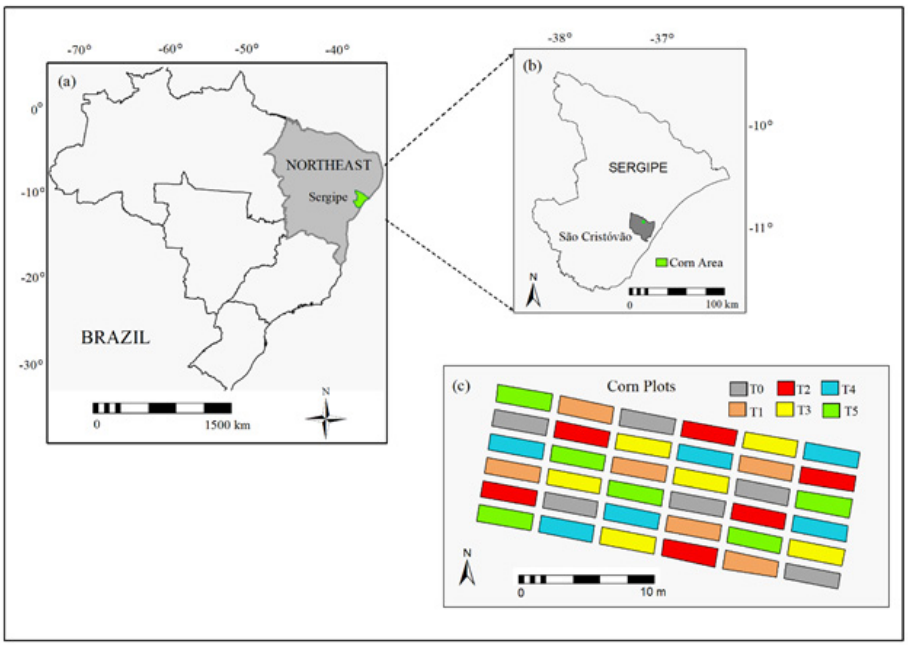

Figure 1: Location of the experimental area. (a) Sergipe in the Northeast Region of Brazil; (b) São Cristóvão County in Sergipe State, and (c) Corn Plots Cover Fertilized with Different Nitrogen (N) Levels from Urea Source, at 0 kg ha^{-1} (T0), 25 kg ha^{-1} (T1), 50 kg ha^{-1} (T2), 100 kg ha^{-1} (T3), 200 kg ha^{-1} (T4), and 400 kg ha^{-1} (T5)

The corn experimental area is the São Cristóvão County, Northeast Brazil, latitude 11° 01′ S, longitude 37° 00′ W, and altitude of 30 m, in a region of tropical sub-humid climate within the Atlantic Forest biome, involving native and anthropized areas but natural species being replaced by rainfed and irrigated annual and perennial crops [32,33]. The long-term annual mean air temperature (T_a) is 25.2 °C, with an annual precipitation (P) of 1331 mm, being rainfall concentrated from March to August. The soil is classified as Red Yellow Argisol, with wavy relief [34].

The general corn sowing time in Sergipe is from the second half of May to the first half of June, with harvest occurring from the second half of October to the first half of November, depending on the cultivar. Following Francelli and Dourado Neto (2000) the corn crop stages (CS) for the SHS 7939 PRO2 cultivar considered in the current research are described in Table 1.

Duration of the Crop Stages – CS (Weeks - W)																		
W/ CS[1]	1	2	3	4	5	6	7	8	9	10	11	12	13	14	15	16	17	18	19
S																			
E																			
V4																			
V6																			
V10																			
PF																			
FF																			
GF																			
PM																			
H																			

Table 1: Crop Stages (CS) for the Rainfed Corn Crop, in the São Cristóvão County, Sergipe State, Northeast Brazil

CS: S – Sowing; E – Emergency; V4, V6, and V10 – Vegetative stages with four, six, and ten leaves, respectively; PF – Pre-flowering; FF – Full flowering; GF – Grain filling; PM– Physiological maturation; H – Harvest.

The experimental design was of random blocks with six repetitions. Sowing (S) time was on 05 Jun 2022, with plots of 8.0 m length composed of 6 lines, plants from the SHS 7939 PRO2 cultivar spaced at 0.5 m between lines, representing a corn cropped area of 864 m^2. The coordinates for all plot vertices were determined using the receptor GNSS Trimble RTK R6, resulting in a mean horizontal error (X and Y) of 0.01 m. Starting from the vertices, polygons were created in GIS QGIS. The average ET_a and BIO values together with their standard deviations (SD) were obtained within the buffered area, at a 0.05 m spatial resolution for each N trial and considered for WP assessments during each CS and for the growing season (GS) (see Figure 1).

Foundation fertilization was at the proportion of 60 and 40 kg ha^{-1} for P_2O_5 and K_2O for all plots, and 35% of the total N applied via urea to each trial. Regarding the experimental trials there were six N cover applications at 0 kg ha^{-1} (T0), 25 kg ha^{-1} (T1), 50 kg ha^{-1} (T2), 100 kg ha^{-1} (T3), 200 kg ha^{-1} (T4) and 400 kg ha^{-1} (T5) at the V4 vegetative CS for the remaining 65% of the N. The harvest was done manually when the grains presented moisture content around 13% and the effects of these different N cover levels on WP in terms of the mo0delling remote sensing BIO were assessed for the drone flights at E, V4, V6, V10, PF, FF and GF crop stages while for the growing season, in terms of BIO and productivity (P_r) field measurements..

Data Collection and Processing

Remote Sensing and Agrometeorological Data

The aerial images were taken during the year 2022 at around 14 UTC (GMT-3) in July 17 (crop stage E), July 28 (crop stage V4), August 04 (crop stage V6), August 18 (crop stage V10), September 01 (crop stage PF), September 13 (crop stage FF), September 22 (crop stage GF), and October 06 (crop stage PM), with a multispectral camera Mapir Survey 3W (Peau Productions, Inc., San Diego, CA, EUA), onboard a drone, using an interface software "Drone Deploy". The mosaic building software was the Agisoft Photoscan 1.3.5, with longitudinal and lateral overlap of 80% and 75%, respectively. Table 2 presents the specifications of the multispectral camera Mapir Survey 3W.

Bands/Image Characteristics				
CentreWavelength (nm)	BandWidth (nm)	FocalLength (mm)	Image Size (Mega Pixels)	Field of View
550	15.0	19.0	4,000 x 3,000	Horizontal: 87.0°
660	15.0			
850	30.0			

Table 2: Specifications of the Multispectral Camera Mapir Survey 3W

Specifications of the multispectral camera Mapir Survey 3W.

With flights at 60 m height, the images are at a 0.05 m spatial resolution. The total drone overflown area was 0.2 ha, covering the studied corn crop, natural vegetation, and bare soil from which the corn plots were cut for WP assessments. The band reflectance values were derived applying an empirical method which is based on a calibration panel by using the software Mapir Camera Control [35].

One agrometeorological station near the experimental area was used for modelling the WP components. The collected agrometeorological data were daily values of incident global solar radiation – R_G; air temperature – T_a (maximum, mean, and minimum values), relative humidity – RH (maximum, mean, and minimum values) and wind speed at a height of 2 m – u_2, which together with remote sensing parameters were inputted for the reference (ET_0) and actual (ET_a) evapotranspiration calculations both considering the Penman-Monteith equation and for biomass production (BIO) by using the RUE Monteith's model [28].

Field Biomass and Grain Measurements

Before harvest, the aerial parts of the corn plants were weighed to obtain fresh matter, and the dry matter was estimated by up scaling a dry sample. One line of each parcel was cut at 20 cm-high from the soil surface and the vegetative material weighed with a manual digital scale. The material was crushed and a representative sample of 400 grams dried in stove with forced air circulation at 65° C until attain a constant weight. The dry matter content was then calculated by the ratio of the dry to the fresh matter of the crushed sample and this ratio multiplied by the total matter, which was considered the field BIO measured to be compared with the BIO retrieved from remote sensing parameters. The grain moisture for each analyzed corn parcel was determined and the productivity (Pr) expressed in kg ha^{-1} after correcting moisture.

Thus, it was also possible to quantify water productivity in terms of Pr – $WP_{Pr,}$ at the crop growing season (GS) timescale. To apply the FAO K_c approach, for detecting water stress conditions, the mean crop height of twelve plants in each corn plot from the soil to the corn cartridges was measured weekly during the FAO mid-season CS, with a three-meter graduate ruler to be used together with wind speed and relative humidity data to estimate K_c value for this CS.

Corn Water Productivity Modelling

Actual Evapotranspiration (Eta) Calculations

The Penman Monteith (PM) equation was applied to acquire ET_a, using agrometeorological and remote sensing data and estimating net radiation (R_n); soil heat flux (G); surface resistance (r_s) and aerodynamic resistance (r_a). The SUREAL model was applied to retrieve r_s and r_a was estimated from roughness parameters [26,27].
According to ET_a (mm d^{-1}) was estimated as:

$$ET_a = \left(\frac{\Delta\left(R_n - G\right) + \frac{\rho_a c_p D}{r_a}}{\Delta + \gamma\left(1 + \frac{r_s}{r_a}\right)} \right) 0.408 \quad [1]$$

where Δ (kPa $°C^{-1}$) is the slope of the saturated vapor pressure curve; R_n (MJ m^{-2} d^{-1}) is the daily net radiation; G is the daily soil heat flux (MJ m^{-2} d^{-1}); ρ_a is air density (kg m^{-3}); c_p is air specific heat at constant pressure (J kg^{-1} K^{-1}); D (kPa) is the vapor pressure deficit; γ is the psychrometric constant (kPa $°C^{-1}$); r_a is the aerodynamic resistance (s m^{-1}); r_s (s m^{-1}) is the surface resistance; and 0.408 is a unit conversion factor [27].

The daily R_n values (W m^{-2}) were estimated throughout the Slob equation

$$R_n = \left(1 - \alpha_0\right) R_G - a_L \tau_{sw} \quad [2]$$

where the regression coefficient a_L was adjusted through its relationship with the mean air temperature; R_G (W m^{-2}) was measured at the agrometeorological station, τ_{sw} is the shortwave transmissivity taken as the ratio of R_G to the solar radiation at the top of the atmosphere (R_{TOP}), with R_{TOP} being obtained by astronomic calculations [3,36]

Regarding the surface albedo (α_0), for each MAPIR band 1 to 3 (Table 2), the solar radiation at the top of the atmosphere was calculated assuming the sun as a blackbody, applying the Planck's law, with the radiation over the wavelength intervals integrated for each wavelength and considering their fractions over the solar spectrum. Then, the broadband α_0 was obtained as the total sum of the narrow-band reflectance values (ρ_b) values according to their weights (w_b) [2].

$$\alpha_0 = \sum w_b \rho_b \quad [3]$$

where the w_b values of 0.42; 0.35; and 0.23, for the Mapir bands 1, 2, and 3, respectively, were the ratio of the amount of the incoming shortwave radiation from the sun at the top of the atmosphere in a particular band and the sum for these bands.

For the ground heat flux (G, MJ m^{-2} d^{-1}) it was estimated according to

$$G = \left[a_G \exp\left(b_G \alpha_0 \right) \right] R_n \quad [4]$$

being R_n in MJ m^{-2} d^{-1}, and a_G and b_G regression coefficients of 3.98 and -25.47, respectively, for the Northeast Brazil [21,26,37].

To estimate r_s (s m^{-1}) the following equation was applied:

$$r_s = \exp\left[a_r \left(\frac{T_0}{\alpha_0} \right) \left(1 - NDVI \right) + b_r \right] \quad [5]$$

where T_0 (°C) is the surface temperature, NDVI is the Normalized Difference Vegetation Index, and the regressions coefficients a and b are 0.04 and of 2.72 for Northeast Brazil [26].
NDVI was calculated from the reflectance values of NIR (ρ_3) and RED (ρ_2) Mapir bands

$$NDVI = \frac{\rho_3 - \rho_2}{\rho_3 + \rho_2} \quad [6]$$

As the MAPIR camera does not have a thermal band, T_0 (K) was retrieved by the residual method applying the Stefan-Boltzmann equation to estimate the long-wave radiation components

$$T_0 = \sqrt[4]{\frac{R_G \left(1 - \alpha_0 \right) + \sigma \varepsilon_a T_a^4 - R_n}{\sigma \varepsilon_0}} \quad [7]$$

where T_a is in K; ε_a is the surface emissivity, σ is the Stefan-Boltzmann constant (5.67 x 10^{-8} W m^{-2} K^{-4}), and ε_0 is the surface emissivity [19,38,39].
The ε_a term from Eq. 7 was acquired as a function of τ_{sw}:

$$\varepsilon_a = a_A \left(\ln \tau_{sw} \right)^{b_A} \quad (8)$$

with a_A and b_A being the regression coefficients, a_A = 0.94 and b_A = 0.10, resulted from field radiation balance measurements in a range of environmental conditions over irrigated crops and natural vegetation in Northeast Brazil [26,37].
The surface emissivity (ε_0) was estimated according to Teixeira et al. (2024):

$$\varepsilon_0 = a_0 \ln(NDVI) + b_0 \quad (9)$$

where a_0 and b_0 being the regression coefficients, a_0 = 0.06 and a_0 = 1.00, resulted from field measurements of the emitted surface radiation and T_0, together with remote sensing calculations of NDVI in Northeast Brazil [26,37].

To estimate the drag force between corn surface and the lower atmosphere, r_a was estimated through the following equation

$$r_a = \frac{\ln\left(\frac{z_m - d}{z_{0m}}\right)\ln\left(\frac{z_h - d}{z_{0h}}\right)}{k^2 u_z} \quad (10)$$

where z_m is the height of wind speed measurements (m), d is the zero plane displacement height (m), z_h is the height of humidity measurements (m), z_{0h} (m) is the roughness length governing transfer of heat and vapor (m), k of 0.41 (-) is the von Karman's constant, and u_z is the wind speed at height z (m s-1). It was assumed d as $4.67z_{0m}$ and z_{0h} being $0.135z_{0m}$, being z_{0m} estimated by:

$$z_{0m} = \exp\left[\left(a_z \frac{NDVI}{\alpha_0}\right) + b_z\right] \quad (11)$$

where a_z and b_z 0.24 and -2.12 are the respective regression coefficients adjusted for Northeast Brazil [26,27]
Eq. 10 is for neutral stability conditions, i.e., where temperature, atmospheric pressure, and wind speed distributions follow nearly adiabatic conditions (no heat exchange). However, as the r_a is in numerator and denominator of Eq. 1, stability corrections are self-canceled with the presence or absence not impacting the final ET_a results under atmospheric instability conditions [26].

Retrieving Biomass Production (BIO) and Water Productivity Based On BIO

For remote sensing BIO (kg ha^{-1} d^{-1}) estimations, the following equation was used according to the physical principle of the Radiation Efficiency Model – RUE

$$BIO = \sum\left(\varepsilon_{max} ET_f PAR_{abs} 0.864\right) \quad (12)$$

where ε_{max} (g MJ^{-1}) is the maximum radiation efficiency use, considered as 3.46 g MJ^{-1} for corn crops the evapotranspiration fraction (ET_f) is the ratio of ET_a to ET_0, PAR_{abs} (W m^{-2}) is the absorbed photosynthetically active radiation, and 0.864 is the unit conversion factor
[6,27,31].

To analyze the effect of the corn root-zone moisture conditions on BIO, the ET_f was included and compared with the potential conditions represented by the FAO K_c approach to detect water stress situations by using the values for the mid station (K_{c_mid}) and fitted a curve for the whole growing season according to

$$K_{c\_mid} = K_{c\_TAB} + \left[0.04\left(u_2 - 2\right) - 0.004\left(RH_{min} - 45\right)\right]\left(\frac{h}{3}\right)^{0.3} \quad (13)$$

Where, for the mid station crop stage, K_{c_TAB} of 1.20 is the tabled crop coefficient for corn crops, u_2 is the average wind speed at 2 m height, RH_{min} is the minimum value of relative humidity, and h is the average crop height [27].

PAR_{abs} (W m^{-2}) is the fraction of the incident photosynthetically active radiation – PAR_{inc} (W m^{-2}), which in turn was considered a percentage of the incident global radiation – R_G (W m^{-2}):

$$PAR_{inc} = a_p PAR_{inc} \quad (14)$$

where a_p is a regression coefficient found to be 0.44 for the Northeast Brazil [37].

$$PAR_{abs} = f_p PAR_{inc} \quad (15)$$

being f_p is calculated as:

$$f_p = a_p NDVI + b_p \quad (16)$$

where a_p and b_p are regression coefficients which in previous study for mixed agroecosystems were estimated respectively as 1.26 and 0.16 [40].

Having remote sensing estimations and field measurements of BIO and field measurements of productivity (Pr), water productivity – WP (kg m^{-3}) was assessed based on both, BIO (kg ha^{-1}) and Pr (kg ha^{-1}):

$$WP_{BIO,Y_a} = \frac{BIO \text{ or } Pr}{ET_a} \quad (17)$$

Statistical Analysis

Besides average pixel values and standard deviations, analyses of variance (ANOVA) were performed using 2-way ANOVA in R (ver. 3.5.1) with a pairwise comparison by applying the Tuckey honestly significant difference (HSD) post-hoc test, to assess differences on water productivity components at 5% significance level, regarding the six N cover fertilizing levels (0 kg ha^{-1}, 25 kg ha^{-1}, 50 kg ha^{-1}, 100 kg ha^{-1}, 200 kg $ha^{-1}$and 400 kg ha^{-1}), and for the drone flights at eight crop stages – CS: Emergency (E), plants with four leaves (V4), plants with six leaves (V6), plants with ten leaves (V10), pre flowering (PF), full flowering (FF), grain filling (GF) and physiological maturation (PM) [2].

Results and Discussion

Weather Water Productivity Drivers

Figure. 2 presents the daily values for daily totals of precipitation – P and reference evapotranspiration – ET_0 (a); and for the daily means of global solar radiation – R_G and air temperature – T_a (b), in terms of Day of the Year – DOY, during the corn growing season in 2022.

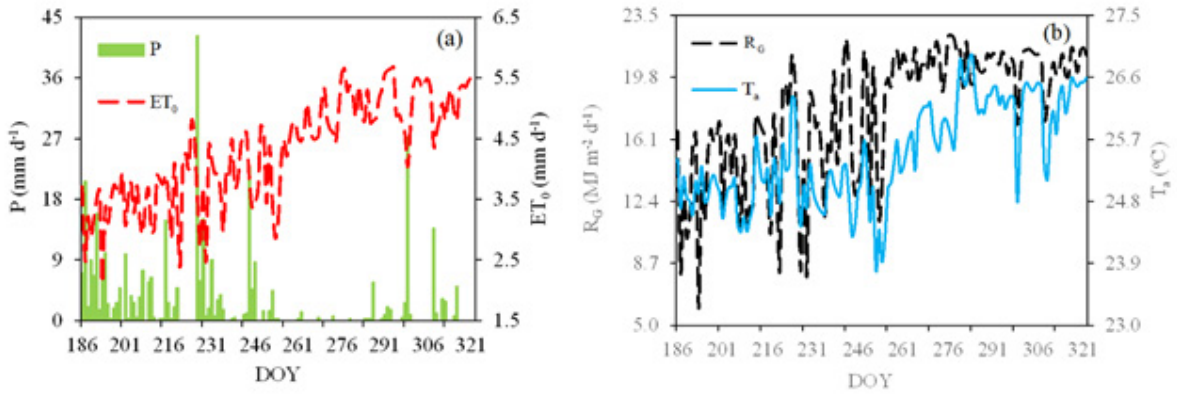

Figure 2: Weather Data During the Corn Growing Season of 2022 in the County of São Cristóvão, Sergipe (SE) State, Northeast Brazil, According to the Day of the Year (DOY). (a) Daily Values for Totals of Precipitation (P) and Reference Evapotranspiration (ET_0); and (b) Daily Mean Values for Global Solar Radiation (R_G) and Air Temperature (T_a)

From Figure. 2_a, rainfall was concentrated between the end of July (DOY 186) and the start of September (DOY 246), when there was the highest P daily value, above 20 mm d^{-1} with a total for the growing season (GS) of 351.4 mm GS^{-1}. ET_0 maximum daily rates were from the beginning of October (DOY 275) to the end of the year, with peaks above 5.5 mm d^{-1} in October (DOY 291-294). Considering the ET_0 for the growing season of 551.6 mm, rainfalls attended only 64% of the atmospheric demand, meaning some water deficit degree in the climatic water balance for the crop, mainly from September (DOY 253) to October (DOY 286).

According to Figure. 2b, R_G and T_a tendencies followed those for ET_0, with respective maximum mean daily values above 20.0 MJ m^{-2} d^{-1} and 26.0 °C from September (DOY 258) to the end of the year; while the corresponding minimum ones, below 15.0 MJ m^{-2} d^{-1} and 20.0 °C were concentrated from the beginning of July (DOY 187) to the end of August (DOY 235). Thus, the best corn root-zone moisture conditions happened from July to September, but under the lowest atmospheric demands, which limited somewhat both ET_a and BIO rates, even under good rainfall-water availability.

Spatial And Temporal Variations In Actual Evapotranspiration – Et_a

Figure. 3 presents the spatial distribution of corn daily ET_a, together with its average pixel values and standard deviations (SD), regarding the whole experimental area and the eight analyzed crop stages – CS in the County São Cristóvão, Sergipe State, Northeast Brazil, during the year 2022.

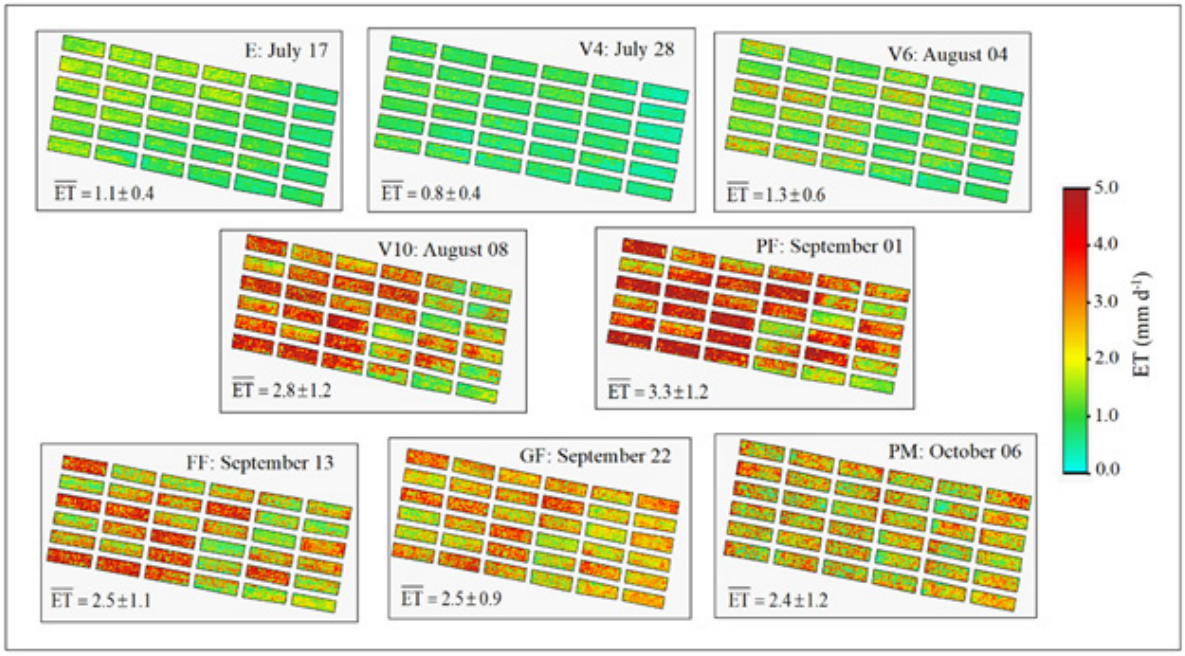

Figure 3: Spatial Distribution of Corn Daily Actual Evapotranspiration (ETa), Together with its Average Pixel Values and Standard Deviations (SD), Regarding the whole experimental area and the eight analyzed corn crop stages – CS, During the year 2022: E – Emergency; V4, V6, and V10 – Vegetative Stages with Four, Six, and Ten Leaves, respectively; PF – Pre-Flowering; FF – Full Flowering; GF – Grain Filling; PM – Physiological Maturation

According to Figure. 3, there was a strong increase on ET_a rates in the whole experimental corn area, along the eight analyzed CS for all N cover fertilizing levels, starting with averages in the range between 0.8 and 1.3 mm d^{-1} from E (July 17) to V6 (August 04), followed by a sharp increase till a mean pixel value of 3.3 mm d^{-1} in PF (September 01), when started to drop to an average of 2.4 mm d^{-1} in PM (October 06). Regarding spatial variations, SD represented 36% (GF – September 22) to 50% (V4 – July 28 and PM – October 06) of the average pixel values.

To assess both ET_a and BIO for each of the six N cover trials (Urea at 0 to 400 kg ha^{-1} N levels, with six repetitions) in each analyzed CS, the average pixel values and SD for the buffered area were used, resulting in around 180,000 pixels for each N cover fertilizing level (see the lower right side of Figure 1).

Table 3 shows ET_a average and SD values from remote sensing measurements, together with the results of the pairwise comparison by group, using the Tuckey HSD post-hoc test performed for the N cover fertilization levels according to each CS.

N levels [1]DOY	CS[2]	T0: 0 (kg ha^{-1})	T1: 25 (kg ha^{-1})	T2: 50 (kg ha^{-1})	T3: 100 (kg ha^{-1})	T4: 200 (kg ha^{-1})	T5: 400 (kg ha^{-1})	Average
198	E	1.12±0.40cd	1.15±0.39d	1.15±0.40c	1.13±0.39d	1.10±0.46de	1.21±0.46de	1.14±0.42
209	V4	0.78±0.34d	0.79±0.34d	0.79±0.34c	0.79±0.37d	0.82±0.44e	0.87±0.46e	0.80±0.38
216	V6	0.95±0.36d	1.08±0.48d	1.19±0.59c	1.31±0.69d	1.50±0.88d	1.54±0.88d	1.26±0.64
230	V10	1.95±0.98ab	2.30±1.12ab	2.73±1.26ab	2.89±1.38ab	3.34±1.42b	3.45±1.33b	2.77±1.24
244	PF	2.17±1.04ab	2.76±1.15a	3.17±1.24a	3.48±1.31a	4.10±1.24a	4.39±1.11a	3.34±1.18
256	FF	1.71±0.88bc	1.90±0.96bc	2.19±1.05b	2.49±1.15bc	3.23±1.23b	3.45±1.11b	2.49±1.06
265	GF	2.19±0.72ab	2.16±0.84ab	2.28±0.83b	2.53±0.88bc	2.96±0.98bc	2.90±0.87bc	2.50±0.85
279	PM	2.47±1.05a	2.18±1.18ab	2.26±1.20b	2.25±1.24c	2.41±1.23c	2.33±1.27c	2.37±1.19
Average	-	1.67±0.72	1.79±0.81	1.97±0.86	2.11±0.93	2.43±0.99	2.52±094	2.08±0.87

Table 3: Average Pixel Values and Standard Deviations (SD) of Actual Evapotranspiration (ETa) from Remote Sensing Measurements, Considering the N Cover Fertilization Levels for each Analyzed Corn Crop Stages (CS), Together with the Tuckey HSD Post-hoc Test Performed by Group

[1]DOY – Day of the Year; [2]CS – Crop stages: E – Emergence; V4 – Vegetative stage with four leaves per plant; V6 – Vegetative stage with six leaves per plant, V10 – Vegetative stage with ten leaves per plant, PF – Reproductive pre flowering, FF – Reproductive full flowering, GF – Reproductive grain filling, and PM – Reproductive physiological maturation. ET_a rates with the same letter in each column indicate no significant differences from each other at 5%.

Table 3 shows strong variations on ET_a from E to PM for each N cover fertilization levels (T0 to T5), evidenced by the Tuckey HSD post-hoc test. The mean daily ET_a rates ranged from a minimum of 0.8 mm d^{-1} from E to V4 in July (DOY 198 to 209 – July 17 to July 28), without significative differences among N cover trials from T0 to T3, increasing to a peak of 4.4 mm d^{-1} for PF (DOY 244, September 01) with T5. Average values for the corn growing season (GS) ranged from 1.7 mm d^{-1} (T0) to 2.5 mm d^{-1} (T5). The high SD values indicated large spatial variations in the root-zone moisture and soil cover conditions, which affected ET_a partitions into transpiration and soil evaporation from canopies and soil, respectively [21,40].

As the ET_a pixel values for each CS and N cover fertilization trial also depended on the climatic water balance, the following analyses considered the accumulated values for precipitation (P_{ac}) and reference evapotranspiration (ET_{0_ac}) between the crop stages, since the seeding time (S), considering the weather data showed in Fig. 2a. From E (July 17, DOY 198) to V4 (July 28, DOY 209), as the soil cover was scarce, there were the lowest ET_a rates, with mean pixel values below 1.3 mm d^{-1} for all N cover fertilizing levels (T0 to T5). During this period, although P_{ac} attended $ET_{0\_ac,}$ with a positive climatic water balance ($P_{ac} – ET_{0\_ac}$ = 44.6 mm) from S (DOY 186, July 05) to V4, there was a higher ET_a partition into soil evaporation. Between V4 and PF (September 01, DOY 244), ET_a rates increased, with averages ranging from 1.0 mm d^{-1} for T0 in V6 (August 04, DOY 216) to 4.4 mm d^{-1} for T5 in PF. During this last period rainfalls still attended the atmospheric demand in the climatic water balance ($P_{ac} – ET_{0\_ac}$ = 8.2 mm), but the soil cover increased contributing to a higher partition of ET_a into transpiration. After PF, ET_a rates dropped till PM (October 06, DOY 279), with general declines in transpiration rates as the harvest stage approached under a negative climatic water balance ($P_{ac} – ET_{0\_ac}$ = -133.0 mm).

The water fluxes were affected by crop development, but according to Tukey's HSD post-hoc test, different for each CS, varying according to the N cover fertilization levels, but not statistically different for the highest ET_a rates between T4 and T5. This is an important issue as for T5, N level 400 kg ha^{-1}, the production cost rises while more N is percolated to the water table increasing environmental negative impacts, comparing with that of 200 kg ha^{-1} (T4). The ET_a rates were most affected by variations on root-zone moisture levels and soil cover, which in turn depend on the weather conditions and CS, affecting the ET_a partitions into transpiration and soil evaporation [42,43]. Considering the evaporative fraction ($ET_f = ET_a/ET_0$) as a corn root-zone moisture indicator crossing ET_0 values (Figure 2a) with the mean ET_a rates (Table 3), it ranged from 0.21 in July (E to V4 CS) from T0 to T3 to above 1.00 in September (PF to FF CS) with T4 and T5 [2]. These ET_f values indicate that, in general, there was no strong water deficit for crop growth along crop stages for N cover fertilizing levels above 200 kg ha^{-1} (T4) and 400 kg ha^{-1} (T5), even with negative water balance ($P – ET_a$) in some circumstances, what could be attributed to a good corn root development promoted by these N cover applications allowing the use of soil moisture at high depths.

reported average corn ET_a rates ranging from 2.0 to 2.8 mm d^{-1} and from 3.1 to 3.8 mm d^{-1} for respectively for rainfed and irrigated conditions in Colorado (USA) [44]. Our average value of 2.1 mm d^{-1} for the corn crop growing season (GS) is inside of their rainfed range. In Northwestern China, modelling and field measurements in irrigated corn crop with mulching retrieved mean ET_a of 3.5 mm d^{-1} close to our averaged value for PF when the plants were at good root-zone rainfall water availability [45]. from drone remote sensing measurements in corn crop growing within the Caatinga Brazilian biome, reported an average ET_a of 2.2 mm d^{-1} under different N cover fertilizin levels with urea [2]. The similarities between our results and those from literature bring confidence in the suitability of estimating ET_a by modelling rs and ra in the Penman-Monteith equation from the reflectance values of the Mapir camera onboard a drone together with agrometeorological data [21,26].

Spatial and Temporal Variations In Biomass Production - Bio

Figgure. 4 presents the spatial distribution of daily corn BIO, together with its average pixel values and standard deviations (SD), regarding the whole experimental area and the eight analyzed crop stages – CS in the County São Cristóvão, Sergipe State, Northeast Brazil, during the year 2022.

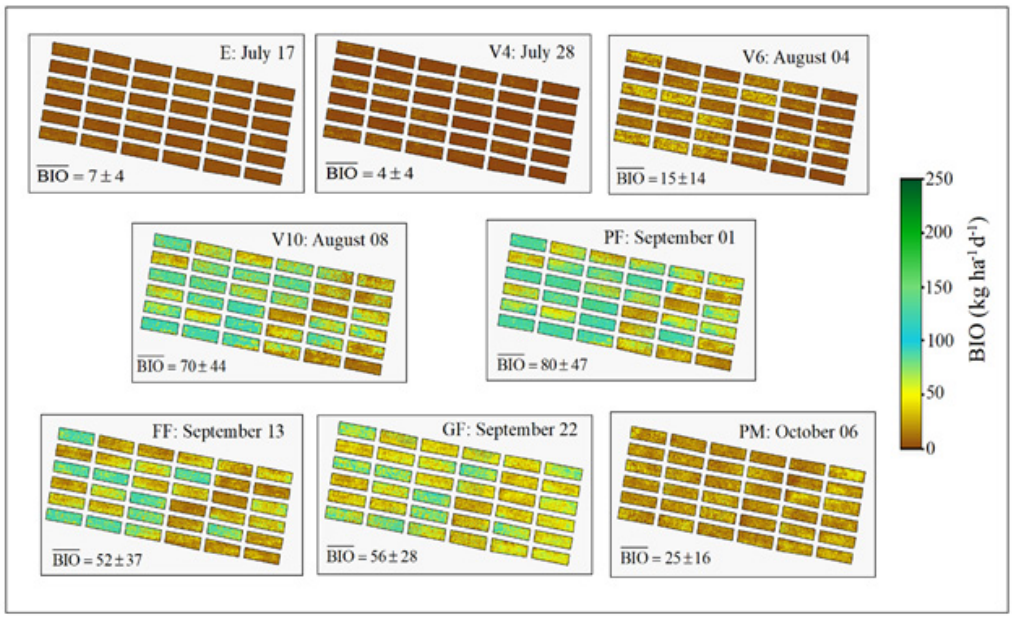

Figure: 4 Spatial Distribution of Daily Biomass Production (BIO), Together With its Average Pixel Values and Standard Deviations (SD), Regarding The Whole Experimental Area and The Eight Analyzed Corn Crop Stages – CS, During The Year 2022: E – Emergency; V4, V6, and V10 – Vegetative Stages With Four, Six, and Ten Leaves, Respectively; PF – Pre-Flowering; FF – Full Flowering; GF – Grain Filling; PM – Physiological Maturation

As for ET_a, there were spatial and temporal BIO variations as shown Fig. 4, for each N cover fertilization level along the corn crop stages (CS), with lower rates from E (July 17) to V6 (August 04), when the mean pixel values ranged from 3 to 10 kg ha^{-1} d^{-1}, followed by an increase till PF (September 01), when the BIO average was 56 kg ha^{-1} d^{-1}, raising 5.6 folds from V6 to PF. After that, BIO dropped to a mean of 18 kg ha^{-1} d^{-1} in PM (October 06). Considering the spatial variations, the highest SD values were in V4 (July 28), representing 100% of the average, and the lowest one, accounting for 40% of the average, happened during GF (September 22).

Table 4 shows BIO averages and SD values from remote sensing measurements, together with the results of the pairwise comparison by group, using the Tuckey HSD post-hoc test performed for the N cover fertilization levels according to each analyzed CS.

N levels / [1]DOY	CS[2]	T0: 0 (kg ha^{-1})	T1: 25 (kg ha^{-1})	T2: 50 (kg ha^{-1})	T3: 100 (kg ha^{-1})	T4: 200 (kg ha^{-1})	T5: 400 (kg ha^{-1})	Average
198	E	5.14±2.90bc	5.83±3.29d	6.77±3.64d	7.35±3.94c	8.42±4.91cd	8.58±4.89de	7.20± 3.93
209	V4	1.52±1.63c	2.14±2.05d	3.24±2.96d	4.22±3.93c	5.97±5.61d	6.10±5.53e	3.87± 3.62
216	V6	5.73±4.27bc	9.55±7.02cd	12.75±9.00d	16.26±12.16c	21.43±16.98cd	22.32±17.39de	14.67± 11.14
230	V10	35.26±25.35a	50.50±30.70a	65.86±36.27a	75.43±41.78a	92.74±46.50ab	98.06±43.11b	69.64± 37.29
244	PF	40.22± 25.54a	54.79±31.86a	67.35±34.07a	81.68±40.24a	108.88±43.17a	123.08±40.70a	79.33±35.93
256	FF	25.18±17.17ab	29.01±18.18bc	35.76±21.83bc	47.88±27.88b	79.51±38.10b	90.99±35.26bc	51.39±26.40
265	GF	41.92±17.01a	42.81±20.4ab	45.83±19.84ab	54.50± 22.88b	76.49±30.59b	75.80±26.21c	56.23±22.82
279	PM	24.91±13.65ab	22.02±14.29bcd	22.80±14.67cd	23.34±15.89c	29.47±17.79c	28.52±18.21d	25.18±15.75
Average	-	22.49±13.44	27.08±15.97	32.55±17.785	38.83±21.09	52.86±25.46	56.68±23.91	38.41±19.61

Table 4: Average Pixel Values and Standard Deviations (SD) of Biomass Production (BIO) From Remote Sensing Measurements, Considering The N Cover Fertilization Levels for Each Analyzed Corn Crop Stages, Together With The Tuckey HSD Post-Hoc Test Performed by Group

[1]DOY – Day of the year; [2]CS – Crop stages: E_ Emergence; V4 – Vegetative stage with four leaves per plant; V6 – Vegetative stage with six leaves per plant, V10 – Vegetative stage with ten leaves per plant, PF – Reproductive pre flowering, FF – Reproductive full flowering, GF - Reproductive grain filling, and PM- Reproductive physiological maturation. BIO rates with the same letter in each column indicate no significant differences from each other at 5%.

According to Table 4, the mean BIO values ranged from a minimum of 1.5 kg ha^{-1} d^{-1} during V4 with T0 (DOY 209, July 28) to a peak of 123.1 kg ha^{-1} d^{-1} in PF (DOY 244, September 01) with T5. However, from the N cover fertilization of 200 kg ha^{-1} d^{-1} (T4) to 400 kg ha^{-1} d_{-1} (T5), there were no significative differences in BIO rates for all CS, with the average for T4 being 93% of that for T5. Regarding the spatial variations, SD values represented between 40% and 106% of

the BIO averages in GF (DOY 265, September 22) with T4 and V4 (DOY 209, July 28) under T0, respectively. The high SD values for corn BIO indicated variabilities in the root-zone moisture and soil cover conditions, as both affect PAR_{abs} [2,21].

From E (July 17, DOY 198) to V4 (July 28, DOY 209), as the soil cover was low, occured the lowest BIO rates, with the lowest mean of 1.5 kg ha^{-1} d^{-1} (V4 in T0), at the respective minimums of 0.03 for fP and 2 W m^{-2} for PAR_{abs}. From V6 (August 04, DOY 216) to PF (September 01, DOY 244), BIO rates increased, with averages surpassing 100 kg ha^{-1} d^{-1} in PF for both T4 and T5. Under these conditions f_p was above 0.35 and PAR_{abs} higher than 30 W m^{-2}. From FF (September 13, DOY 256) to PM (October 06, DOY 259), BIO rates dropped, reaching a mean below 25 kg ha^{-1} d^{-1} for T0 to T3 in PM, promoted by declines on f_p lower than 0.20 for T0 to T2 as the harvest time approached, even with mean PAR_{abs} values still above 20 W m^{-2} during this CS.

The reproductive crop stages presenting the maximum BIO rates, agree with who reported highest values of remote sensing vegetation indices when the corn canopies fully covered the soil [11,46]. In addition, the R_G increases in September favored the photosynthetic activity, which together crop development raising PAR_{abs}, brought the BIO peaks in the current paper, corroborating with [47]. According to transpiration rates favoring photosynthetic activities, increase BIO, under good root-zone moisture levels. [48, 49] In the current research, BIO followed the development of leaf areas with increases of ET_a partition into transpiration which in turn is related to soil cover and corn crop stages [2,21,43, 50]. Using remote sensing measurements, showed relationships between BIO and transpiration in corn crops under both irrigation and rainfed conditions, confirming that energy partition into soil evaporation does not contribute to BIO. through remote sensing measurements with a Sequoia camera onboard drone in corn crop N cover fertilized with urea within the Caatinga Brazilian biome, reported larger BIO rates ranging from 40 kg ha^{-1} d^{-1} in V6 for N level of 0 kg ha^{-1} to 228 kg ha^{-1} d^{-1} for FF with N applications at 200 kg ha^{-1} [2,51,52]. One of the reasons for these last larger BIO rates compared to our results is that, besides being a different cultivar growing in a distinct biome, there were higher both P and R_G levels during these crop stages in their study, promoting deeper root systems to explore larger soil moisture volumes.

Water productivity dynamics

Table 5 presents the WP_{BIO} averages and SD values from remote sensing measurements, together with the results of the pairwise comparison by group, using the Tuckey HSD post-hoc test performed for the N cover fertilization levels according to each analyzed CS.

N levels / [1]DOY	[2]CS	T0: 0 (kg ha^{-1})	T1: 25 (kg ha^{-1})	T2: 50 (kg ha^{-1})	T3: 100 (kg ha^{-1})	T4: 200 (kg ha^{-1})	T5: 400 (kg ha^{-1})	Average
198	E	0.48±0.25de	0.53±0.27de	0.60±0.25de	0.66±0.27d	0.76±0.28c	0.71±0.28c	0.62±0.27
209	V4	0.20±0.19e	0.27±0.22e	0.38±0.24e	0.48±0.29d	0.63±0.33c	0.61±0.31c	0.43±0.26
216	V6	0.59±0.31d	0.83±0.34cd	1.01±0.35c	1.14±0.42c	1.27±0.49b	1.29±0.46b	1.02±0.40
230	V10	1.70± 0.57ab	2.10±0.53a	2.33±0.55e	2.52±0.55a	2.68±0.55a	2.79± 0.47a	2.35±0.54
244	PF	1.82±0.67ab	1.98±0.70ab	2.12±0.67a	2.31±0.69ab	2.62±0.61a	2.79±0.60a	2.27±0.66
256	FF	1.58±0.87b	1.71±0.94b	1.76±0.86b	2.02±0.89b	2.48±0.80a	2.68±0.76a	2.04±0.85
265	GF	1.93±0.48a	2.02±0.60ab	2.04±0.56ab	2.18±0.56ab	2.58±0.55a	2.63±0.52a	2.23±0.55
279	PM	1.09±0.50c	1.14± 0.60c	1.14±0.59c	1.18±0.63c	1.33±0.60b	1.36±0.66b	1.21± 0.60
Average	-	1.17 ± 0.48	1.32 ± 0.53	1.42 ± 0.51	1.56 ± 0.54	1.79 ± 0.53	1.86 ± 0.51	1.52 ± 0.51

Table 5: Average Pixel Values and Standard Deviations (SD) of Water Productivity Based on Biomass Production (WPBIO) From Remote Sensing Measurements, Considering The N Cover Fertilization Levels For Each Analyzed Corn Crop Stages, Together With The Tuckey HSD Post-Hoc Test Performed by Group

[1]DOY – Day of the year; [2]CS – Crop stages: Emergence; V4 – Vegetative stage with four leaves per plant; V6 – Vegetative stage with six leaves per plant, V10 – Vegetative stage with ten leaves per plant, PF – Reproductive pre flowering, FF – Reproductive full flowering, GF - Reproductive grain filling, and PM- Reproductive physiological maturation. WP_{BIO} values with the same letter in each column indicate no significant differences from each other at 5%.

From Table 5, the mean WP_{BIO} values ranged from an average of 0.2 kg m^{-3} during V4 for T0 (July 28, DOY 209) to a peak of 2.8 kg m^{-3} from V10 (August 18, DOY 230) to PF (September 01, DOY 244) with T5. However, as for BIO, from the N cover fertilizing of 200 kg ha^{-1} d^{-1} (T4) to 400 kg ha^{-1} d^{-1} (T5), there were no significative differences considering all crop stages, with the average for T4 being 94% of that for T5. Regarding the spatial variations, SD represented between 21% and 100% of the average WP_{BIO} in GF (September 22, DOY 265) with T4 and in V4 with T0, respectively.

During the period from E (July 17, DOY 198) to V4, the BIO low rates (Table 4), even with low ET_a (Table 3) generated the minimum WP_{BIO} values, with a mean ranging from 0.2 kg m^{-3} (T0) to 0.6 kg m^{-3} (T4 and T5) during this CS. WP_{BIO}

increased from V6 (August 04, DOY 216) attaining an average of 2.8 kg m_{-3} between V10 (August 19, DOY 230) and PF (September 01, DOY 256) with both T4 and T5. Under these last conditions the high mean BIO rates ranged from 93 to 123 kg ha^{-1} d^{-1}, while the corresponding ones for ET[a] were from 3.3 to 4.4 mm d^{-1}. WP_{BIO} values dropped to a mean value of 1.1 kg m^{-3} from T0 to T3 in PM, when ET_a and BIO reached mean pixel values below 2.3 mm d^{-1} and 23 kg ha^{-1} d^{-1}, respectively.

According to the WP_{BIO} values, there were variations among N cover fertilization trials due to root-zone moisture, crop development, and solar radiation levels. However, considering the six repetitions for each N cover fertilization trials, it is clearly noticed from the statistical analyses, that with N at 200 kg ha^{-1} (T4), should be a best option when aiming good corn yields while saving water and money, besides avoiding environmental problems with much N leaching to the ground water under higher applications rates. reported higher WP_{BIO} values, above 4.0 kg m^{-3}, during the V10 and PF corn crop stages for N cover fertilization at 200 kg ha^{-1} with urea, due to larger BIO rates when compared with those for the current study. [2] However, the authors mentioned the same effects for both nitrate and urea N sources in corn crops cultivated in the Caatinga Brazilian biome, but in this case, the WP_{BIO} stabilization occurred at N cover fertilization with 150 kg ha^{-1}.

Remote sensing estimations versus field measurements

Figure. 5 was built to analyze the effect of soil moisture conditions on water productivity components for each of the N cover fertilization levels and to give more confidence for ET_a and BIO modelling results, by comparing the ET_f values which represent the true root-zone moisture status with the FAO crop coefficient (K_c) ones which picture the potential conditions of water fluxes [10,53].

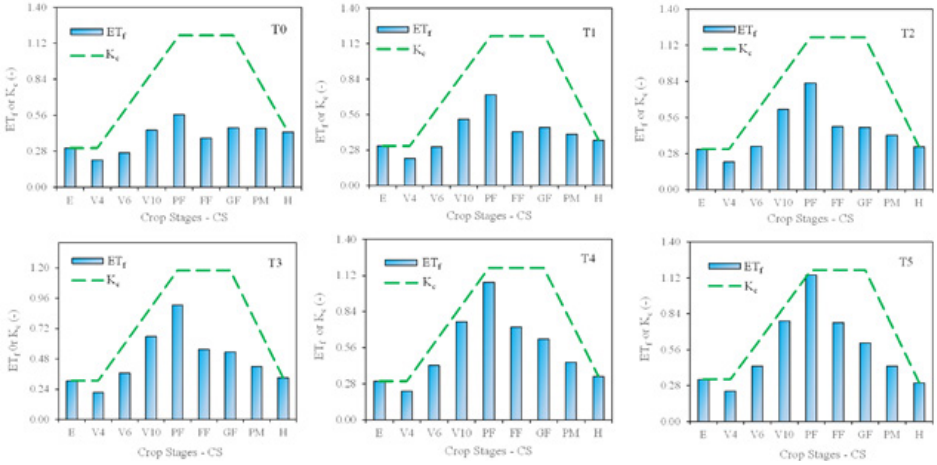

Figure 5: Evaporative Fraction (ET_f) and FAO Crop Coefficient (K_c) Along The Corn Crop Stages (CS) For Each of N Cover Fertilization Level.
N levels – T0: N Cover at 0 kg ha^{-1}; T1: N Cover at 25 kg ha^{-1}; T2: N Cover at 50 kg ha^{-1}; T3: N Cover at 100 kg ha^{-1}; T4: N Cover at 200 kg ha^{-1}; and T5: N Cover at 400 kg ha^{-1}
CS – E: Emergency; V4, V6 and V10: Corn Plants With Four, Six and Ten Leaves, Respectively; PF: Pre Flowering; FF: Full Flowering; GF: Grain Filling; PM: Physiological Maturation; and H: Harvest

The ET_f values are the ratios of actual (ET_a) to reference (ET_0) evapotranspiration, while K_c is the ratio of potential evapotranspiration (ET_p) to ET_0 [21]. For the FAO K_c approach the lengths of crop development stages were adjusted to a growing season of 140 days growing in California (USA) [27]. With this adjustment the length of the mid-season (mid) coincided with the period from pre flowering (PF) to grain filling (GF) for the current study. The K_{c_mid} was estimated by Eq. 13 and the curves in Fig. 5 were constructed considering the K_{c_ini} (initial stage) and K_{c_end} (end stage) values being the same as those for ET_f estimated from remote sensing measurements together with agrometeorological data for the E and H crop stages, respectively, considering each N cover fertilization level. As for the H stage it wasn´t carried out drone flights, a relation ET_f with accumulated degree-days was used for K_{c_end} [2]. Field measured of corn heights (h) varied from 1.20 m (T0) to 1.90 m (T5) but this h range didn't alter the K_{c_mid} from the mean value of 1.18 for all N cover levels, a little lower than the FAO tabled value of 1.20 for non-stressed, well-managed corn crops under subhumid climates.

The ET_f values bellow K_c after the corn FF stage, even with N cover above 200 kg ha^{-1}, indicated some degrees of water stress during each CS, which should have affected somewhat the WP components, mainly for N cover fertilization at 0 kg ha^{-1} (T0) and 50 kg ha_{-1} (T1) [4,10,53,56]. However, for T4 and T5, the K_c curve followed well the ET_f values till PF (September 01, DOY 244), what means that the cover fertilizations above 200 kg ha^{-1} favor the corn root systems to use water at deeper soil depths under lower water availability (see also Fig. 2a), bringing more confidence for the sensitivity of the SUREAL algorithm for estimating ET_a. The assumption of equal values for ET_f and K_c during the E and H crop

stages for all N cover fertilization trials is plausible, as in the E stage there was a very high soil exposed and in the H stage plants were under senescence conditions. In both situations plants were with transpiration rates close to zero [2].

Field measurements of biomass production (BIO_{FM}) and corn grain productivity (Pr_{FM}) allowed to check the relations of field measured (FM) and remote sensing estimated (RS) parameters, considering all the analyzed CS and N cover fertilization levels for the GS (Figure 6).

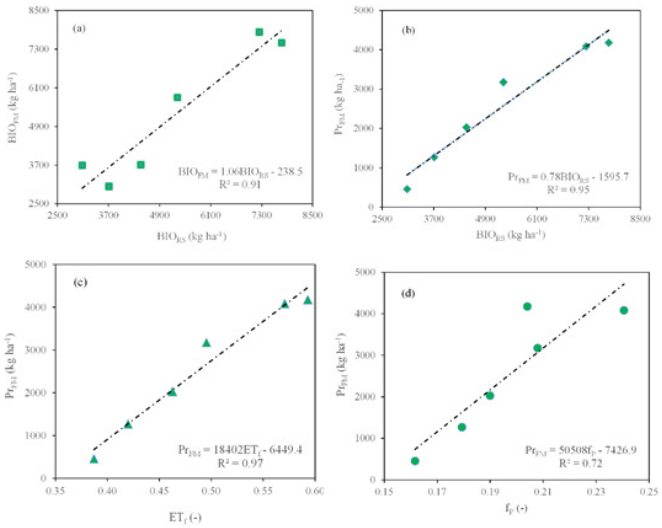

Figure 6: Relations Between Field Measurements (FM) and Remote Sensing Modelling (RS) For the Corn Growing Season (GS): (a) Biomass Production From Field Measurements (BIOFM) and From Remote Sensing Modelling (BIO_{RS}); (b) Field Measured Productivity (Pr_{FM}) and BIORS, (c) Pr_{FM} and Evapotranspiration Fraction (ET_f); and (d) Pr_{FM} and Fraction of The Absorbed Photosynthetically Active Radiation (f_p)

From Figure. 6a, it can be noticed, by the high determination coefficient (R^2 = 0.91), comparing field measurements (BIO_{FM}) with remote sensing results (BIO_{RS}), the robustness of the joining the SUREAL the RUE models to estimate BIO. Even higher correlation (R^2 = 0.95) was obtained with field measured productivity (Pr_{FM}) and BIO_{RS} (Figure 6b). Among the remote sensing parameters, the highest correlation for P_{rFM} was with ET_f (R^2 =0.97), presented in Fig. 6c, but with a still high R^2 of 0.80 for f_p (Figure 6d). These results show that ET_f has the strongest effect on corn plants growth, but f_p also influences their vigor through photosynthetic activity. Yet, the importance of the relation depicted on Fig. 6c is that BIO can be estimated from measurements of crop ET_a and ET_0 from an agrometeorological station and on Fig. [10,21] 6d is that BIO can also be retrieved with field measurements with reasonably accuracy placing solar radiation sensors above and below the corn canopies along the growing seasons [30].

To analyze the suitability of productivity (Pr) estimations through vegetation vigor before harvest (H), Figure. 7 shows the relations of Pr_{FM} and BIO_{RS} from crop stages V6 (plants with six leaves) to PM (Physiological Maturation).

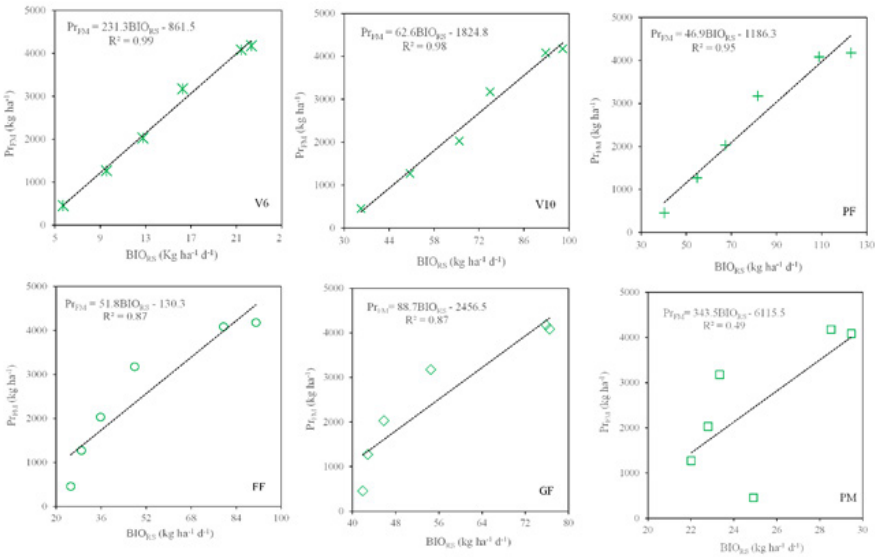

Figure 7: Relation Between Field Measured Productivity (Pr_{FM}) and The Remote Sensing Modelled Biomass Production (BIO_{RS}) For Different Corn Crop Stages. The Vegetative Stages, V6 and V10, Plants With Six and Ten Leaves, Respectively; and The Reproductive Stages, PF - Flowering; FF - full Flowering; GF - Grain Filling, PM – Physiological Maturation

According to Figure. 7 correlations between growing season field Pr and daily remote sensing BIO measurements declined when the crop stages went from V6 to PM. The importance of the highest determination coefficient during V6 (R^2 = 0.99) is that corn yield can be accurately predicted allowing guiding farmers about post-harvest processes. The low determination coefficient on PM stage (R^2 = 0.49) evidence that yield had been already defined in V6, what agrees with Fancelli and Dourado Neto (2000), who pointed out that the crop on this CS defines the potential productivity for corn crop. The similarity of the remote sensing BIO, and field measured P_r brings additional confidence for the modelling, compensating somewhat for the need of advanced expensive energy and carbon balance towers for validations, allowing reliable remote sensing comparisons among different N cover fertilization levels for the rainfed corn crop.

Growing Season Water Productivity Components

Having productivity data available (Pr) (weight of grains per ha) for each N cover fertilization trial, besides WP_{BIO}, it was also possible to carry out WP_{Pr} assessments for the growing season (GS). The averaged ET_f for each N cover fertilization levels were multiplied by ET_0 resulting in GS ET_a values, while the mean f_p values were used to estimate GS BIO with R_G data and remote sensing parameters. Thus, with the GS values of BIO_{RS}, BIO_{FM}, and P_{rFM}, the values for WP_{BIO_RS}, WP_{BIO_FM} and WP_{Pr_FM} were assessed applying Eq. 17 (Table 6).

WP component[1]/ N treatment[2]	ET_a (mm)	BIO_{RS} (kg ha^{-1})	BIO_{FM} (kg ha^{-1})	Pr_{FM} (kg ha^{-1})	WP_{BIO_RS} (kg m^{-3})	WP_{BIO_FM} (kg m^{-3})	WP_{Pr} (kg m^{-3})
T0	228.0	3,080.4	3,697.1	455.9	1.35	1.62	0.20
T1	245.2	3,710.1	3,040.8	1,271.2	1.51	1.24	0.52
T2	269.9	4,458.7	3,713.7	2,029.5	1.65	1.38	0.75
T3	289.0	5,320.0	5,800.0	3,175.4	1.84	2.01	1.10
T4	333.3	7,242.3	7,830.7	4,085.1	2.17	2.35	1.23
T5	344.9	7,765.3	7,499.0	4,178.0	2.25	2.17	1.21
Mean	285.1	5,262.8	5,105.4	2,532.5	1.85	1.85	0.89

Table 6: Corn Growing Season (GS) Values For Water Productivity (WP) Components

[1]ET_a – Actual Evapotranspiration; BIO_{RS} – Biomass Production from remote sensing parameters; BIO_{FM} – Biomass Production from field measurements; P_{rFM} – Corn productivity from field measurements; WP_{BIO_RS} – Water Productivity based on BIO_{RS}; WP_{BIO_FM} – Water Productivity based on BIO_{FM}, and WP_{Pr} – Water Productivity based on P_{rFM}. [2]T0 – 0 N cover; T1: N cover at 25 kg ha^{-1}; T2: N cover at 50 kg ha^{-1}; T3: N cover at 100 kg ha^{-1}; T4: N cover at 200 kg ha^{-1}; T5: N cover at 400 kg ha^{-1}. The highest GS ET_a was for the N cover fertilization level of 400 kg ha^{-1} (T5), 51% above that for T0 (no N cover fertilizing). The largest GS values for BIO_{RS} and P_r were also for T5, but these differences were not significantly from those for T4 (7% for BIO_{RS} and only 2% for P_{rFM}), while for BIO_{FM} the value for T4 was 4% higher than that for T5 but probably also influenced by the sampling processes. The similarity between BIO_{RS} and BIO_{FM} generated the same average values of 1.85 kg m^{-3} for WP_{BIO_RS} and WP_{BIO_FM} two times of the mean WP_{Pr}.

As for BIO, WP values stabilized after the N cover fertilizing level of 200 kg ha^{-1} (T4). The average WP_{BIO_RS} values from Table 6 are higher than that found by of 0.97 kg m^{-3} in Tanzania, but these last authors attributed this low value to poor corn yields under rainfed conditions in their study region [9]. However from satellite measurements, reported an average WP_{BIO_RS} of 2.10 kg m^{-3} for rainfed corn crop growing under the conditions of the Brazilian Cerrado biome within Central West region, while for pivot irrigated corn, found average WP_{Pr} of 2.00 kg m^{-3} within this same biome, but in Southeast Brazil [1,57]. Lower WPBIO and WP_{Pr} in the Brazilian Atlantic Forest biome for the current study can be explained by less water availability in the corn root zones under rainfall water deficit conditions during the study period.

The harvest index (HI), i.e. the ratio of P_r to BIO, ranged from 0.12 for BIO_{FM} with T0 to 0.60 with T3 and T4 for BIO_{RS}. This HI range agrees with who reported HI values from 0.20 to 0.56 for corn under different growing conditions in South Romania, and those from 0.37 to 0.55 for rainfed corn cover fertilized with nitrate and urea in the Caatinga Brazilian Biome found average corn ET_a, P_r and BIO respective values of 331 mm, 3,200 kg ha^{-1}, and 6,800 kg ha^{-1} for a rainfed corn growing season, yielding an average HI of 0.47, using Sentinel and Landsat 8 images in the north-eastern part of Tanzania. However, this last study involved different CS at the same time and pixel contaminations with other crops. [2,9,58].

Considering the corn grain prices in 2022, the WP_{Pr} monetary vales were around US$0.20 m^{-3} with the recommended N cover fertilization level of 200 kg ha^{-1} (T4), which is lower than those for irrigated corn within the Brazilian Cerrado biome (0.34 to 0.68 US$ m^{-3}) reported by corn crop under rainfed conditions in the Brazilian Caatinga biome, around 0.50 US$ m^{-3} but like those for other arable crops around the world (0.10 to 0.20 US$ m^{-3}) However, reasons for these differences can be attributed, besides methods, to distinct cultivars and environmental conditions. [1,2,59]

Conclusions

Reflectance measurements from a camera onboard a drone in the ranges of visible and near infra-red bands together with weather data, dry matter and yield field data, allowed the rainfed corn water productivity assessments at high spatial resolution, with detections of the effect of N cover fertilizations. Distinct actual evapotranspiration (ET_a) and biomass production (BIO) rates promoted different water productivity (WP) values for each crop stage (CS), with peaks during the reproductive stages from pre flowering (PF) to grain filling (GF) but stabilizing for all CS at N levels of 200 kg ha^{-1}. This means that with N cover fertilizations above this level will promote money losses and increase risks of negative environmental impacts with more N leaching to the water table.

Relations of measured productivity (Pr) with remote sensing parameters showed that its best correlation was with the evaporative fraction (ET_f), but the fraction of the absorbed photosynthetically active radiation (f_p) had its influence through photosynthetic activity. Comparing Pr with remote sensing modeled BIO (BIO_{RS}), the highest determination coefficient at V6 (plant with six leaves) indicated that corn yield can be predicted during this specific CS, guiding farmers about post-harvest processes. Applications of the remote sensing models showed that they are useful for monitoring vegetation and water conditions in corn crops with aerial camera onboard drone, allowing rational fertilization practices while maintained yield at low water use. Although the methods were tested in a specific crop growing region of the Atlantic Forest Brazilian biome, they success of the methods showed strong potential to support sustainable agriculture. Limitations for applications in other environments could be the probable need of local calibrations for the modelling equations by simultaneous field and remote sensing measurements.

References

1. de Castro Teixeira, A. H., Hernandez, F. B. T., Andrade, R. G., Leivas, J. F., de Castro Victoria, D., & Bolfe, E. L. (2014). Irrigation performance assessments for corn crop with Landsat images in the São Paulo state, Brazil. Water Resources and Irrigation Management-WRIM, 3(2), 91-100.
2. Teixeira, A., Pacheco, E., Silva, C., Dompieri, M., & Leivas, J. (2021). SAFER applications for water productivity assessments with aerial camera onboard a remotely piloted aircraft (RPA). A rainfed corn study in Northeast Brazil. Remote Sensing Applications: Society and Environment, 22, 100514.
3. Luns Hatum de Almeida, S., Brunno Costa Souza, J., Furlan Nogueira, S., Ricardo Macedo Pezzopane, J., Heriberto de Castro Teixeira, A., Bosi, C., ... & Pereira da Silva, R. (2023). Forage mass estimation in silvopastoral and full sun systems: Evaluation through proximal remote sensing applied to the SAFER model. Remote Sensing, 15(3), 815.
4. de Paula Almeida, F., Junior, J. A., Knapp, F. M., Fernandes Souza, J. M., de Castro Teixeira, A. H., Evangelista, A. W. P., ... & Battisti, R. (2025). Impacts of corn flowering on estimation of evapotranspiration using remote sensing in Brazilian Savanna. Australian Journal of Crop Science, 19(4), 378-387.
5. Bakhsh, A., Jaynes, D. B., Colvin, T. S., & Kanwar, R. S. (2000). Spatio-temporal analysis of yield variability for a corn-soybean field in Iowa. Transactions of the ASAE, 43(1), 31-38.
6. Bayma, G., Nogueira, S. F., Adami, M., Sano, E. E., Nunez, D. C., Santos, P. M., ... & Skakun, S. (2025). Estimating forage mass in Brazilian pasture-based livestock production systems through satellite and climate data integration. Computers and Electronics in Agriculture, 237(11049), 6.
7. Ko, J., & Piccinni, G. (2009). Corn yield responses under crop evapotranspiration-based irrigation management. Agricultural water management, 96(5), 799-808.
8. Liu, J., Pattey, E., Miller, J. R., McNairn, H., Smith, A., & Hu, B. (2010). Estimating crop stresses, aboveground dry biomass and yield of corn using multi-temporal optical data combined with a radiation use efficiency model. Remote Sensing of Environment, 114(6), 1167-1177.
9. Nyolei, D., Nsaali, M., Minaya, V., van Griensven, A., Mbilinyi, B., Diels, J., ... & Kahimba, F. (2019). High resolution mapping of agricultural water productivity using SEBAL in a cultivated African catchment, Tanzania. Physics and Chemistry of the Earth, Parts A/B/C, 112, 36-49.
10. Venancio, L. P., Mantovani, E. C., Amaral, C. H. D., Neale, C. M. U., Filgueiras, R., Gonçalves, I. Z., & Cunha, F. F. D. (2020). Evapotranspiration mapping of commercial corn fields in Brazil using SAFER algorithm. Scientia Agricola, 78(4), e20190261.
11. Zhang, L., Niu, Y., Zhang, H., Han, W., Li, G., Tang, J., & Peng, X. (2019). Maize canopy temperature extracted from UAV thermal and RGB imagery and its application in water stress monitoring. Frontiers in plant science, 10, 1270.
12. Sah, R. P., Chakraborty, M., Prasad, K., Pandit, M., Tudu, V. K., Chakravarty, M. K., ... & Moharana, D. (2020). Impact of water deficit stress in maize: Phenology and yield components. Scientific reports, 10(1), 2944.
13. Batistoti, J., Marcato Junior, J., Ítavo, L., Matsubara, E., Gomes, E., Oliveira, B., ... & Dias, A. (2019). Estimating pasture biomass and canopy height in Brazilian savanna using UAV photogrammetry. Remote Sensing, 11(20), 2447.
14. Maes, W. H., & Steppe, K. (2019). Perspectives for remote sensing with unmanned aerial vehicles in precision agriculture. Trends in plant science, 24(2), 152-164.
15. Manfreda, S., McCabe, M. F., Miller, P. E., Lucas, R., Pajuelo Madrigal, V., Mallinis, G., ... & Toth, B. (2018). On the use of unmanned aerial systems for environmental monitoring. Remote sensing, 10(4), 641.
16. Tunca, E., Köksal, E. S., Çetin, S., Ekiz, N. M., & Balde, H. (2018). Yield and leaf area index estimations for sunflower plants using unmanned aerial vehicle images. Environmental monitoring and assessment, 190(11), 682.
17. Colaço, A. F., & Bramley, R. G. (2018). Do crop sensors promote improved nitrogen management in grain crops?. Field Crops Research, 218, 126-140.
18. Sharma, L. K., & Bali, S. K. (2017). A review of methods to improve nitrogen use efficiency in agriculture. Sustainability,

10(1), 51.
19. Silva, C. D. O. F., de Castro Teixeira, A. H., & Manzione, R. L. (2019). Agriwater: An R package for spatial modelling of energy balance and actual evapotranspiration using satellite images and agrometeorological data. Environmental modelling & software, 120, 104497.
20. Teixeira, A., Leivas, J., Takemura, C., Bayma, G., Garçon, E., Sousa, I., ... & Silva, C. (2023). Remote sensing environmental indicators for monitoring spatial and temporal dynamics of weather and vegetation conditions: applications for Brazilian biomes. Environmental Monitoring and Assessment, 195(8), 944.
21. de Castro Teixeira, A. H., Leivas, J. F., Takemura, C. M., Pacheco, E. P., Garçon, E. A. M., de Sousa, I. F., ... & Santos, A. F. M. (2024). Modeling and Monitoring Water Productivity by Using Geotechnologies: In Some Brazilian Agroecosystems. In Remote Sensing Handbook, Volume V (pp. 383-421). CRC Press.
22. Togeiro de Alckmin, G., Kooistra, L., Rawnsley, R., & Lucieer, A. (2021). Comparing methods to estimate perennial ryegrass biomass: Canopy height and spectral vegetation indices. Precision Agriculture, 22(1), 205-225.
23. Nagler, P. L., Glenn, E. P., Nguyen, U., Scott, R. L., & Doody, T. (2013). Estimating riparian and agricultural actual evapotranspiration by reference evapotranspiration and MODIS enhanced vegetation index. Remote Sensing, 5(8), 3849-3871.
24. Senay, G. B., Schauer, M., Friedrichs, M., Velpuri, N. M., & Singh, R. K. (2017). Satellite-based water use dynamics using historical Landsat data (1984–2014) in the southwestern United States. Remote Sensing of Environment, 202, 98-112.
25. Vanino, S., Nino, P., De Michele, C., Bolognesi, S. F., D'Urso, G., Di Bene, C., ... & Napoli, R. (2018). Capability of Sentinel-2 data for estimating maximum evapotranspiration and irrigation requirements for tomato crop in Central Italy. Remote Sensing of Environment, 215, 452-470.
26. Teixeira, A. H. D. C. (2010). Determining regional actual evapotranspiration of irrigated crops and natural vegetation in the São Francisco river basin (Brazil) using remote sensing and Penman-Monteith equation. Remote Sensing, 2(5), 1287-1319.
27. Allen, R. G., Pereira, L. S., Raes, D., & Smith, M. (1998). Crop evapotranspiration-Guidelines for computing crop water requirements-FAO Irrigation and drainage paper 56. Fao, Rome, 300(9), D05109.
28. Monteith, J. L. (1977). Climate and the efficiency of crop production in Britain. Philosophical transactions of the royal society of London. B, Biological Sciences, 281(980), 277-294.
29. Claverie, M., Demarez, V., Duchemin, B., Hagolle, O., Ducrot, D., Marais-Sicre, C., ... & Dedieu, G. (2012). Maize and sunflower biomass estimation in southwest France using high spatial and temporal resolution remote sensing data. Remote Sensing of Environment, 124, 844-857.
30. Tesfaye, K., Walker, S., & Tsubo, M. (2006). Radiation interception and radiation use efficiency of three grain legumes under water deficit conditions in a semi-arid environment. European journal of Agronomy, 25(1), 60-70.
31. Tollenaar, M., Bruulsema, T. W., 1988. Efficiency of maize dry matter production during periods of complete leaf area expansion. Agron. J. 80,580-585.
32. Ribeiro, M. C., Metzger, J. P., Martensen, A. C., Ponzoni, F. J., & Hirota, M. M. (2009). The Brazilian Atlantic Forest: How much is left, and how is the remaining forest distributed? Implications for conservation. Biological conservation, 142(6), 1141-1153.
33. Procopio, S. D. O., Cruz, M. A. S., de Almeida, M. R. M., de Jesus Junior, L. A., Nogueira Junior, L. R., & de Carvalho, H. W. L. (2019). Sealba: região de alto potencial agrícola no Nordeste brasileiro.
34. BOMFIM, L. F. C., COSTA, I. V. G. D., & BENVENUTI, S. M. P. (2002). Projeto cadastro da infra-estrutura hídrica do Nordeste. Estado de Sergipe. Diagnóstico do município de Salgado. CPRM.
35. Smith, G. M., & Milton, E. J. (1999). The use of the empirical line method to calibrate remotely sensed data to reflectance. International Journal of remote sensing, 20(13), 2653-2662.
36. De Bruin, H. A. R., & Stricker, J. N. M. (2000). Evaporation of grass under non-restricted soil moisture conditions. Hydrological sciences journal, 45(3), 391-406.
37. de Castro Teixeira, A. H., Bastiaanssen, W. G., Ahmad, M. U. D., Moura, M. D., & Bos, M. G. (2008). Analysis of energy fluxes and vegetation-atmosphere parameters in irrigated and natural ecosystems of semi-arid Brazil. Journal of Hydrology, 362(1-2), 110-127.
38. Peters, A. J., Walter-Shea, E. A., Ji, L., Vina, A., Hayes, M., & Svoboda, M. D. (2002). Drought monitoring with NDVI-based standardized vegetation index. Photogrammetric engineering and remote sensing, 68(1), 71-75.
39. Ramírez-Cuesta, J. M., Vanella, D., Consoli, S., Motisi, A., & Minacapilli, M. (2018). A satellite stand-alone procedure for deriving net radiation by using SEVIRI and MODIS products. International journal of applied earth observation and geoinformation, 73, 786-799.
40. Bastiaanssen, W. G., & Ali, S. (2003). A new crop yield forecasting model based on satellite measurements applied across the Indus Basin, Pakistan. Agriculture, ecosystems & environment, 94(3), 321-340.
41. Villalobos, F. J., Testi, L., Orgaz, F., García-Tejera, O., Lopez-Bernal, A., González-Dugo, M. V., ... & Fereres, E. (2013). Modelling canopy conductance and transpiration of fruit trees in Mediterranean areas: a simplified approach. Agricultural and forest meteorology, 171, 93-103.
42. Fandiño, M., Cancela, J. J., Rey, B. J., Martínez, E. M., Rosa, R. G., & Pereira, L. S. (2012). Using the dual-Kc approach to model evapotranspiration of Albariño vineyards (Vitis vinifera L. cv. Albariño) with consideration of active ground cover. Agricultural Water Management, 112, 75-87.
43. Rosa, R. D., Ramos, T. B., & Pereira, L. S. (2016). The dual Kc approach to assess maize and sweet sorghum transpiration and soil evaporation under saline conditions: Application of the SIMDualKc model. Agricultural Water

Management, 177, 77-94.
44. DeJonge, K. C., Ascough Ii, J. C., Andales, A. A., Hansen, N. C., Garcia, L. A., & Arabi, M. (2012). Improving evapotranspiration simulations in the CERES-Maize model under limited irrigation. Agricultural water management, 115, 92-103.
45. Ding, R., Kang, S., Li, F., Zhang, Y., & Tong, L. (2013). Evapotranspiration measurement and estimation using modified Priestley–Taylor model in an irrigated maize field with mulching. Agricultural and Forest Meteorology, 168, 140-148.
46. Taghvaeian, S., Chávez, J. L., & Hansen, N. C. (2012). Infrared thermometry to estimate crop water stress index and water use of irrigated maize in Northeastern Colorado. Remote Sensing, 4(11), 3619-3637.
47. Yang, Y., Xu, W., Hou, P., Liu, G., Liu, W., Wang, Y., ... & Li, S. (2019). Improving maize grain yield by matching maize growth and solar radiation. Scientific reports, 9(1), 3635.
48. Driscoll, S. P., Prins, A., Olmos, E., Kunert, K. J., & Foyer, C. H. (2006). Specification of adaxial and abaxial stomata, epidermal structure and photosynthesis to CO2 enrichment in maize leaves. Journal of experimental botany, 57(2), 381-390.
49. Kang, S., Zhang, F., Hu, X., & Zhang, J. (2002). Benefits of CO2 enrichment on crop plants are modified by soil water status. Plant and soil, 238(1), 69-77.
50. Longo-Minnolo, G., Vanella, D., Consoli, S., Intrigliolo, D. S., & Ramírez-Cuesta, J. M. (2020). Integrating forecast meteorological data into the ArcDualKc model for estimating spatially distributed evapotranspiration rates of a citrus orchard. Agricultural Water Management, 231, 105967.
51. Campos, I., Neale, C. M., Arkebauer, T. J., Suyker, A. E., & Gonçalves, I. Z. (2018). Water productivity and crop yield: A simplified remote sensing driven operational approach. Agricultural and Forest Meteorology, 249, 501-511.
52. Twohey III, R. J., Roberts, L. M., & Studer, A. J. (2019). Leaf stable carbon isotope composition reflects transpiration efficiency in Zea mays. The Plant Journal, 97(3), 475-484.
53. Lu, N., Chen, S., Wilske, B., Sun, G., & Chen, J. (2011). Evapotranspiration and soil water relationships in a range of disturbed and undisturbed ecosystems in the semi-arid Inner Mongolia, China. Journal of Plant Ecology, 4(1-2), 49-60.
54. Liao, C., Wang, J., Dong, T., Shang, J., Liu, J., & Song, Y. (2019). Using spatio-temporal fusion of Landsat-8 and MODIS data to derive phenology, biomass and yield estimates for corn and soybean. Science of the total environment, 650, 1707-1721.
55. Trout, T. J., & DeJonge, K. C. (2017). Water productivity of maize in the US high plains. Irrigation Science, 35(3), 251-266.
56. Wang, Y., Janz, B., Engedal, T., & de Neergaard, A. (2017). Effect of irrigation regimes and nitrogen rates on water use efficiency and nitrogen uptake in maize. Agricultural Water Management, 179, 271-276.
57. Teixeira, A. H. D. C., Victoria, D. C., Andrade, R. G., Leivas, J. F., Bolfe, E. L., & Cruz, C. R. (2014, October). Coupling MODIS images and agrometeorological data for agricultural water productivity analyses in the Mato Grosso state, Brazil. In Remote Sensing for Agriculture, Ecosystems, and Hydrology XVI (Vol. 9239, pp. 278-291). SPIE.
58. Ion, V., Dicu, G., Dumbravă, M. A. R. I. N., Temocico, G. E. O. R. G. E. T. A., Alecu, I. N., Băşa, A. G., & State, D. A. N. I. E. L. (2015). Harvest index at maize in different growing conditions. Romanian Biotechnological Letters, 20(6), 10951-10960.
59. Sakthivadivel, R., De Fraiture, C., Molden, D. J., Perry, C., & Kloezen, W. (1999). Indicators of land and water productivity in irrigated agriculture. International Journal of Water Resources Development, 15(1-2), 161-179.